Journal of Applied Polymer Science

Direct-current conductivity at a cryogenically low temperature for polymer/carbon composites: Applicability of different theoretical models

Ali Aldalbahi,[1] Mostafizur Rahaman,[1] Tapan Kumar Chaki,[2] Dipak Khastgir[2]
[1]Department of Chemistry, College of Science, King Saud University, Riyadh 11451, Saudi Arabia
[2]Rubber Technology Centre, Indian Institute of Technology Kharagpur, Kharagpur, India
Correspondence to: A. Aldalbahi (E-mail: aaldalbahi@ksu.edu.sa) and D. Khastgir (E-mail: khasdi@rtc.iitkgp.ernet.in)

ABSTRACT: In this study, we focused on the behavior of the direct-current (dc) conductivity/resistivity in a cryogenically low temperature region (10–300 K) for ethylene vinyl acetate copolymer, acrylonitrile butadiene copolymer, and their 50/50 blend composites filled with different conductive carbons. The composites were prepared through a melt-mixing technique. Different behaviors of the dc resistivity/relative resistivity for the composites were observed; these behaviors depended on the nature of the polymers, the filler types, and the filler concentration when plotted with respect to the temperature. The results of dc conductivity were fitted with some existing theoretical models, including Arrhenius, Kivelson, and Mott's variable range hopping, to check their applicability for these composite systems. We observed that none of the models was applicable within the entire range of measurement temperatures but were confined within limited temperature ranges. The reason behind the nonapplicability of the models is discussed with consideration of their drawbacks and limitations. © 2016 Wiley Periodicals, Inc. J. Appl. Polym. Sci. **2016**, *133*, 43541.

KEYWORDS: composites; conducting polymers; theory and modeling

Received 12 November 2015; accepted 13 February 2016
DOI: 10.1002/app.43541

INTRODUCTION

The change in the direct-current (dc) resistivity against temperature in cryogenically low temperature regions has been found to be quite different from the variation of the dc resistivity against temperature in high-temperature regions for conductive polymer composites.[1] In higher temperature regions, the conductivity of composites depends significantly on the matrix polymer behavior, but in a low-temperature region, especially below the glass–rubbery transition temperature, the conductivity of composites is mainly influenced by the conductive additives.[2] Costa and Henry[2] studied the low-temperature (80–250 K) electrical conductivity of polystyrene carbon black composites where the concentration of carbon black in the polystyrene matrix was below the electrical percolation threshold. They fitted the data in Mott's three-dimensional variable range hopping (VRH) model and found that their results were in good agreement with this model. They calculated the average hopping distance, active center density, and associated energy.

The low-temperature electronic transport behavior of poly(vinyl alcohol)/silver nanocomposites was investigated in the temperature range 77–300 K.[3] We observed that the variation of conductivity was marginal up to 150 K, and thereafter, there was a sharp increase in the conductivity up to 300 K. All of the composites exhibited semiconducting behavior because of the charge transfer between poly(vinyl alcohol) and silver with increasing temperature. The conductivity results of the composites were also well fitted with Mott's VRH three-dimensional model up to a certain temperature range. Bahrami *et al.*[4] studied the Hall effect and electrical conductivity in the temperature region 100–300 K for polypyrrole carbon nanotube composites. The conductivity increased with increasing temperature for all of the composites under investigation. The electrical conductivity of the composites also showed good fitting with Mott's three-dimensional VRH model. The charge carrier density increased increasing temperature, whereas the mobility decreased. They attributed the fact that the increase in conductivity was due to increase in temperature to the dominant effect of the charge carrier concentration (n).

Likewise, the behavior of the dc resistivity/conductivity below room temperature of organic and inorganic semiconductors/conductors and composites was studied by several authors in the past, and efforts were made to justify the applicability of different existing theoretical models in the experimental results of conductivity.[5–12] However, to the best of our knowledge, the study of the low-temperature electrical transport behaviors of polymer composite materials having different polymers and

Table I. General Specifications of the Conductex Carbon Black, Printex Carbon Black, and SCF

Typical property	Conductex	Printex	SCF	Unit
Mean particle size	20	35	—	nm
Average filament length	—	—	6	mm
Filament diameter	—	—	0.0068	mm
Surface area, STSA	125	587	—	m^2/g
Surface area, CTAB	130	600	—	m^2/g
Aspect ratio (length/diameter)	—	—	882	—
DBP absorption	115	350–410	—	cc/100 g
Volatiles at 105 °C	1.5	1.0	—	%

[a] *STSA* statistical thickness surface area; *CTAB* cetyl trimethyl ammonium bromide; *DBP* dibutyl phthalate.

their blends filled with different conductive additives has rarely been done; this left us with a great scope for this study.

Previously, we studied the electromagnetic interference shielding effectiveness and high-temperature dc resistivity of ethylene vinyl acetate copolymer (EVA), acrylonitrile butadiene rubber (NBR), and their blend composites filled with Conductex carbon black, Printex carbon black, and short carbon fibers (SCFs).[13–15] In this study, we dealt with the temperature-dependent dc resistivity/conductivity in a cryogenically low-temperature region (10–300 K) for the same polymers, EVA and NBR, and their 50/50 blend composites filled with the same carboneous additives, Conductex and Printex carbon blacks and SCFs. A Hall effect study was carried out to calculate *n*, the Hall mobility (μ), and the drift velocity (V_d). The applicability of different theoretical models defining the temperature-dependent electrical conductivity was also tested to check the applicability of these composites.

EXPERIMENTAL

Materials and Methods

The base polymer matrixes were NBR (Mooney viscosity ML_{1+4} at 100 °C = 45), with an acrylonitrile content of 33%, which was supplied by Japan Synthetic Rubber Co., Ltd., and EVA (EVA-2806; Mooney viscosity ML_{1+4} at 100 °C = 20), with a vinyl acetate content of 28% (melt flow index = 6), which was purchased from NOCIL (Mumbai, India). The conductive fillers, Conductex carbon black (supplied by Columbian Chemicals Co., Atlanta), Printex XE2 carbon black (procured from Degussa Canada, Ltd.), and conductive SCFs (RK 30/12, obtained from RK Carbon Fiber, Ltd., UK), were used in the preparation of the composites. Table I shows the characteristics of all three types of carbon fillers.

The curing agent, dicumyl peroxide (DCP; melting point = 80 °C, purity = 98%), was supplied by Aldrich Chemical Co. (United States). Triallyl cyanurate (TAC; supplied by E. Merck India, Ltd.) was used as a covulcanizing agent. The antioxidant, 1,2-dihydro-2,2,4-trimethyl quinoline (TQ; polymerized), was obtained from Lanxess India Private, Ltd.

The blending of EVA with NBR to make different composites was done with a Brabender plasticorder (PLE 330) at 120 °C for 6 min at 60 rpm in all cases. The ejected heated material was then passed through a two-roll mill to obtain a flat shape. Conductex carbon black or Printex carbon black was mixed with the blending compositions in a two-roll mill, where the other ingredients (TAC, TQ, and DCP) were added in a sequential manner according to the formulation given in Table II. Similarly, the SCFs were mixed with the neat EVA, neat NBR, and their 50/50 blend along with other ingredients in a Haake Rheocord instrument with the same processing conditions and sequence mentioned earlier. A Monsanto R-100S rheometer was used to determine the optimum cure time at 160 °C for 1 h for these composites. The test samples were prepared in an electrically heated press at 160 °C under an identical pressure of 5 MPa. In an example of composite nomenclature, $E_{50}N_{50}P_{10}$ indicates a blend composition of 50/50 w/w EVA/NBR containing 10 parts of Printex-grade conductive carbon black by weight and so on. Similarly, Conductex carbon black and Short carbon fiber are abbreviated as C and F, respectively. In these formulations, all ingredients were taken as parts by weight per hundred parts by weight of polymer (php).

Testing and Characterization

The dc resistivity at cryogenic temperatures (10–300 K) was measured by the Vander Pauw four-probe technique with the help of a dc source meter (Keithley, model 220) coupled with a dc multimeter (Keithley, model 2182). The temperature was controlled by a Lakeshore temperature controller (model 331) with the help of liquid helium (Sumitomo Cryogenics, model HC-4E). The following sample dimensions were used during the measurement: length = 1 cm, width = 0.6 cm, and sample thickness (b) $\approx$ 0.1 cm. The method was based on the application of a current (I) and the measurement of voltage (V). The

Table II. Formulations of the EVA/NBR Composites

	Composition (php)		
Ingredient	E_0N_{100}	$E_{50}N_{50}$	$E_{100}N_0$
EVA	0	50	100
NBR	100	50	0
DCP	02	02	02
TAC	01	01	01
TQ	01	01	01
Conductex carbon black	60	30, 60	60
Printex carbon black	30	30, 50	30
SCF	20	20, 30	20

I–V characteristics at low temperature were also measured by this technique, where *I* was varied over a specified range, and the V corresponded to that applied *I*.

The Hall properties of the different composites were measured with a Hall effect instrument (Lake Shore magnet power supply, model 662). The Vander Pauw technique was used to measure the Hall voltage (U_H) when a definite *I* was passed through the conductor at magnetic fields (*B*s) of 0 and 4000 gauss (Lake Shore model 450 Gauss meter). *n*, μ, and V_d were calculated with the following formulas:

$$n = IB/qb|U_H|$$

$$\mu = |U_H|/R_sIB = 1/(qnbR_s)$$

$$V_d = I/nqab$$

where *q* is the elementary charge (1.602×10^{-19} C), R_s is the sheet resistance, and *a* is the width of the sample.

The dynamic mechanical analysis of the composites was studied with a TA Instruments 2980 V1.7B series instrument. The samples were tested in tension film mode, where the constant frequency was 1 Hz, the amplitude was 10 μm, and the static force was 0.01 N. The temperature was varied from −70 to 70 °C at a scan rate of 3 °C/min in a liquid nitrogen environment.

RESULTS AND DISCUSSION

dc Resistivity against Temperature in the Different Blend Compositions

Insulating polymers can be made electrically conducting by the addition of conductive additives within its matrixes.[16,17] After a certain loading, a continuous conductive network of filler particles is formed within the polymer matrix, where a drastic change in the electrical conductivity/resistivity is observed. This is known as the *percolation threshold* of electrical conductivity/resistivity. Before this percolation threshold value (at a lower loading of filler), the conductive additives remain isolated from each other within the polymer matrix. At this stage, the conductivity is mostly governed by the nature of the polymer matrix, and hence, there is marginal variation in the conductivity with increasing cryogenic temperature. However, around and above the percolation threshold value, the conductive additives remain close to each other within the polymer matrix. As a result, the charge carriers can hop easily from one conductive site to another, and there is sharp variation in the conductivity with increasing temperature. This is because the conductivity is mostly governed by the characteristics of the fillers beyond their percolation threshold value. Hence, in this study, we chose composites that had electrical conductivity/resistivity around and above the percolation threshold value.

The variation of the dc resistivity over the temperature range 10–300 K for the composites based on neat EVA and neat NBR and their 50/50 blend matrixes filled with Conductex carbon black, Printex carbon black, and SCFs is presented in Figure 1. We observed in Figure 1(a) that qualitatively, the nature of the variation of the dc resistivity against temperature for the three matrix polymers was almost the same. The dc resistivity sharply decreased from 10 K to around 60 K, and thereafter, the change in resistivity was found to be marginal for all of the systems up

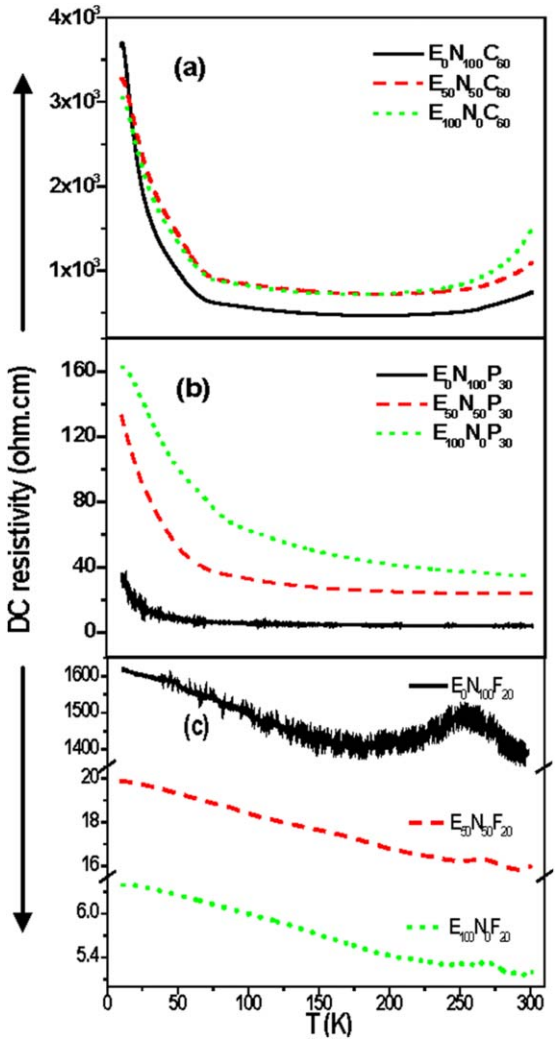

Figure 1. dc resistivity versus temperature for the (a) $E_0N_{100}C_{60}$, $E_{50}N_{50}C_{60}$, and $E_{100}N_0C_{60}$; (b) $E_0N_{100}P_{30}$, $E_{50}N_{50}P_{30}$, and $E_{100}N_0P_{30}$; and (c) $E_0N_{100}F_{20}$, $E_{50}N_{50}F_{20}$, and $E_{100}N_0F_{20}$ composites. [Color figure can be viewed in the online issue, which is available at wileyonlinelibrary.com.]

to 250 K. However, when the temperature was increased further beyond 250 K, there was again some tendency for the resistivity to increase with increasing temperature up to 300 K (the maximum measurement temperature for this experiment). The neat EVA and EVA/NBR (50/50) blend composites showed almost similar values for resistivity and also trends in the temperature dependency of the resistivity above 10–250 K, whereas the composite based on neat NBR showed a somewhat lower resistivity at all temperatures compared to the composites based on the EVA and EVA/NBR blend. However, when the conductive additive was changed from Conductex black to Printex black, some distinct differences in the magnitude of resistivity for the three base polymer matrixes were observed, and the order of resistivity was as follows: EVA > EVA/NBR blend > NBR [Figure 1(b)]. The trend in the variation of the resistivity against temperature was, however, similar to that observed for Conductex black. The resistivity was found to decrease sharply with increasing temperature from 10 to 100 K for the composite based on neat EVA,

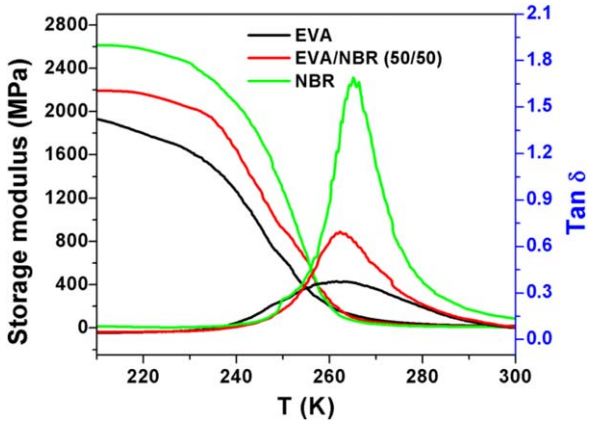

Figure 2. Storage modulus and tan δ versus temperature for EVA, NBR, and their 50/50 blend. [Color figure can be viewed in the online issue, which is available at wileyonlinelibrary.com.]

10 to 70 K for the EVA/NBR (50/50) blend composite, and 10 to 50 K for the neat NBR composite. The variation of the dc resistivity against temperature for the SCF-filled composites was, however, distinctly different from those of the particulate composites of Conductex black and Printex black [Figure 1(c)]. Unlike the carbon black composites, for the SCF-filled composites, the dc resistivity continuously decreased with increasing temperature above 10–200 K for neat NBR and 10–250 K for the composites based on the EVA/NBR (50/50) blend and neat EVA. The plot of the dc resistivity against temperature showed a distinct peak in the case of the pure NBR composites, whereas the plots showed a relatively weak peak in the EVA/NBR (50/50) blend and the neat EVA composites. This indicated that initially, an negative temperature coefficient (NTC) effect was observed for all of the systems followed by a positive temperature coefficient (PTC) effect, which led to peak formation. The existence of a peak at temperatures above 250 K, precisely at a temperature of 270 K, may have been due to some kind of thermally induced motion of the polymer chain. This temperature corresponded to the glass-transition temperature for EVA and NBR, as shown by the dynamic mechanical analysis plots (Figure 2). In fact, the PTC effect was observed for composites containing Conductex black above 250 K; this may have also been due to this molecular motion of the polymer chain around the glass-transition temperature.

When we compared the change in the relative resistivity against temperature, a very similar observation was made for the composites filled with Conductex black and Printex black. The relative resistivity was defined as ρ_t/ρ_0, where ρ_t is the resistivity at any temperature and ρ_0 is the resistivity at the starting temperature, which was 10 K. The variations of the relative resistivity versus temperature for different composites (shown in Figure 3) were similar to the corresponding resistivity versus temperature plots. A careful look at Figure 3 reveals that the neat NBR composites exhibited a higher change in the relative resistivity; this behavior was followed by the 50/50 blend composites and neat EVA composites for Conductex and Printex black filled composite systems. We also observed that the change in the relative resistivity for the fiber-filled neat NBR composite was the lowest up to 160 K, but after that, a large hump was observed; this may have been due to its lowest polymer–filler interaction[14] and highest damping behavior (Figure 2). The appearance of this large hump deviated from its trend for the overall change in the relative resistivity, as observed for the Conductex and Printex black filled NBR composites.

dc Resistivity against Temperature at Different Filler Loadings

The variation of the dc resistivity and relative resistivity against temperature (10–300 K) for the EVA/NBR (50/50) blend filled with Conductex and Printex carbon black and SCFs are shown in Figures 4 and 5. We observed from these plots, especially from Figure 5, that the composites having lower filler loadings exhibited higher degrees of change in the relative resistivity against temperature plots compared to composites with higher loadings of the same type of filler. At and above room temperatures, three different types of mechanisms were proposed for electrical conduction in extrinsically conductive composites; these were electric field radiation, hopping/tunneling of electrons, and electron conduction through particle–particle contact.[18] However, at very low temperatures, the electrical conduction was proposed to be due to the hopping/tunneling of electrons from one conducting site to another. With increasing filler loading in the polymer matrixes, the average interparticle distance/gap decreased along with the increase in the number of conductive networks in the system. Thus, the possibility of conduction through physical contact and hopping was much greater in composites having filler loadings substantially higher than the percolation threshold. In such composites, the effect of the temperature on the variation in resistivity was also less pronounced. However, the composite having filler loadings closer to the percolation threshold had higher interparticle gaps and only a few continuous conductive networks. As a result, the effects of the temperature on the change in the average gap and the change in the conductive network either by formation or

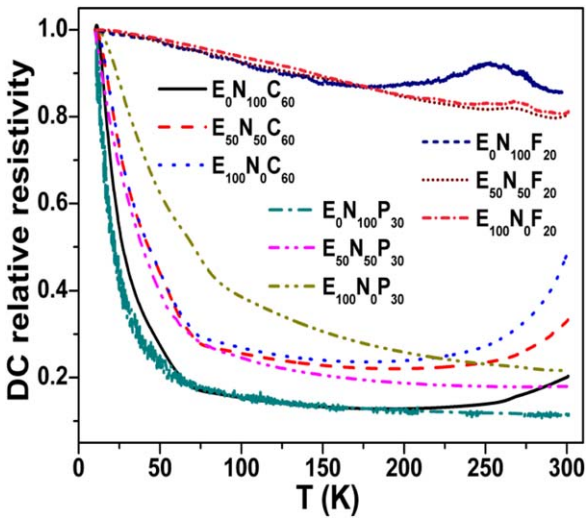

Figure 3. dc relative resistivity versus temperature for the $E_0N_{100}C_{60}$, $E_{50}N_{50}C_{60}$, $E_{100}N_0C_{60}$, $E_0N_{100}P_{30}$, $E_{50}N_{50}P_{30}$, $E_{100}N_0P_{30}$, $E_0N_{100}F_{20}$, $E_{50}N_{50}F_{20}$, and $E_{100}N_0F_{20}$ composites. [Color figure can be viewed in the online issue, which is available at wileyonlinelibrary.com.]

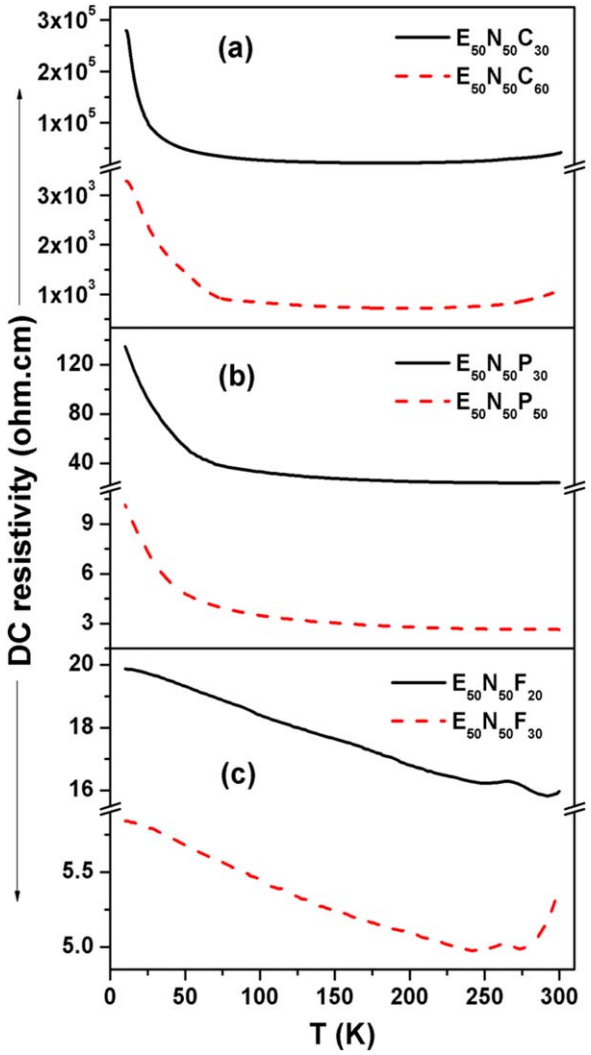

Figure 4. dc resistivity versus temperature for the (a) $E_{50}N_{50}C_{30}$ and $E_{50}N_{50}C_{60}$, (b) $E_{50}N_{50}P_{30}$ and $E_{50}N_{50}P_{50}$, and (c) $E_{50}N_{50}F_{20}$ and $E_{50}N_{50}F_{30}$ composites. [Color figure can be viewed in the online issue, which is available at wileyonlinelibrary.com.]

destruction were significantly large. Moreover, at the lowest measurement temperature, the kinetic energy associated with electrons was much lower, and when the average gap among the particles was high, the possibility of electron hopping was also less. So, the composite system having less conductive filler exhibited a higher change in resistivity. However, with increasing temperature, the possibility of electron hopping increased and resistivity decreased, and the effect became more pronounced in the composites with lower loadings compared to the one with a higher loading.

The change in the relative resistivity versus temperature was also influenced by the nature of the carbon particles. When we looked at the plots of the composites $E_{50}N_{50}C_{30}$, $E_{50}N_{50}P_{30}$, and $E_{50}C_{50}F_{30}$ in Figure 5, with filler loadings of 30 phr, we observed that the changes in the relative resistivity were 1–0.1, 1–0.2, and 1–0.86, respectively. Thus, the change in the relative resistivity for the carbon fell in the order Conductex black > Printex black > SCF. This revealed that the high structure/aspect ratio carbons exhibited less change in the relative resistivity when measured against the temperature.

The temperature coefficient of resistivity (TCR) gave us an idea with respect to the variation of electrical resistivity with temperature. We determined this with the following relation[19]:

$$\mathrm{TCR} = \left[\frac{1}{\rho(T_1)}\right]\left[\frac{\rho(T_2)-\rho(T_1)}{T_2-T_1}\right] \quad (1)$$

where $\rho(T_2)$ and $\rho(T_1)$ are the resistivities at temperatures T_2 and T_1, respectively. The calculated TCR values of $E_{50}N_{50}C_{60}$, $E_{50}N_{50}P_{30}$, and $E_{50}N_{50}F_{30}$ composites are shown in Table III. As shown in Table III, the negative values of TCR were observed in lower temperature ranges, and positive values of TCR were observed in higher temperature ranges. Actually, the electrical resistivity was controlled by the hopping of charge carriers (electrons) from one discrete conductive aggregate to another. The hopping of electrons reduced the electrical resistivity. However, the probability of electron hopping depended on the interparticle gap, which was controlled by the differential thermal expansion of the matrix polymer and conductive aggregates. At very low temperatures, the polymer molecular motion was completely frozen, and the effect of differential thermal expansion between matrix polymer and filler aggregates was also negligible. So, the conduction was mainly due to the hopping of electrons in localized sites. Moreover, the hopping distance was very small; this could be easily covered by the electrons with its available kinetic energy, even at very low temperatures. This was the reason that with increasing temperature from 10 to 60 K, an increased thermal activation of the charge carrier with increasing temperature in the cryogenic range caused a sharp increase in the conductivity, that is, a reduction in the resistivity. However, when the temperature went beyond a limit, this thermal activation energy (E_a) and energy to cross the hopping gap almost balanced each other over a wide temperature range when a marginal change in the resistivity against temperature

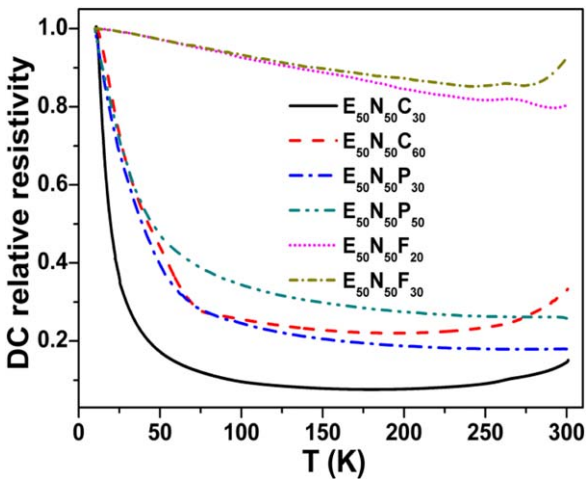

Figure 5. dc relative resistivity versus temperature for the $E_{50}N_{50}C_{30}$, $E_{50}N_{50}C_{60}$, $E_{50}N_{50}P_{30}$, $E_{50}N_{50}P_{50}$, $E_{50}N_{50}F_{20}$, and $E_{50}N_{50}F_{30}$ composites. [Color figure can be viewed in the online issue, which is available at wileyonlinelibrary.com.]

Table III. TCR Values of the $E_{50}N_{50}C_{60}$, $E_{50}N_{50}P_{30}$, and $E_{50}N_{50}F_{30}$ Composites

	Calculated TCR value		
Temperature range	$E_{50}N_{50}C_{60}$	$E_{50}N_{50}P_{30}$	$E_{50}N_{50}F_{30}$
10-50	−0.01370876	−0.01511677	−0.00068493
50-100	−0.00863367	−0.00758124	−0.00080986
100-150	−0.00224731	−0.00325655	−0.00074862
150-200	−0.00066240	−0.00176296	−0.00056805
200-250	0.00134747	−0.00080155	−0.00043457
250-275	0.00491685	−0.00025249	0.00001404
275-300	0.01058522	0.00022420	0.00331299

was observed. However, in higher temperature ranges, especially above the glass-transition temperature, where positive values of TCR were observed, the electrical resistivity was mostly governed by the thermal expansion. This led to a marginal increase in the resistivity with increasing temperature.

Hall Effect Study

The *Hall effect* is described as the voltage difference (U_H) generated across an electrical conductor transverse to an electric I when a B is applied perpendicular to the direction of I. For negatively charged carriers, such as electrons in metal or a dopant in n-type semiconductors, U_H is negative, whereas for positive charge carriers, such as electron holes in p-type semiconductors, U_H is positive. The Hall effect measurement provides information about the type of charge carrier present in the system and values of n, μ, and V_d. The variation of n, μ, V_d, and the product of n and μ ($n \times \mu$) with temperature are plotted in Figure 6 for the composites $E_{50}N_{50}C_{60}$, $E_{50}N_{50}P_{50}$, and $E_{50}N_{50}F_{30}$. We observed from these figures that all of these parameters were temperature-dependent. It is generally observed that with increases in both n and μ, there is an increment in the resistivity. However, we observed for these systems that initially, with increasing temperature, n increased; this was followed by a marginal decrease, whereas μ and V_d were found to decrease initially followed by increases after they attained minima. However, plots of $n \times \mu$ against temperature showed that the trend of variation was similar to that of the n versus temperature plots [Figure 6(c)]. So, we inferred that the resistivity at low temperature was influenced more by n than by its μ.

Applicability of Different Models to dc Conductivity versus Temperature

Arrhenius Model. Although the Arrhenius equation is mostly used to explain the variation of the electrical conductivity with respect to high temperature, here we tested this equation to check its applicability in a low-temperature region. The equation based on this model is given as follows[7];

$$\sigma(T) = \sigma_0 e^{\left(\frac{-E_a}{kT}\right)} \tag{2}$$

or

$$\ln \sigma = \ln \sigma_0 - \frac{E_a}{kT} \tag{3}$$

where σ is the conductivity at temperature T, σ_0 is the pre-exponential factor/limiting conductivity at infinite temperature, and k is Boltzmann's constant ($k \approx 8.617 \times 10^{-5}$ eV/K). Equation (3) reveals that the plot of ln σ against $1/T$ should be a straight line. The Arrhenius plots of the composites with different carbon fillers and blend compositions are presented in Figures 7 and 8, respectively. We observed from these figures that the linearity was not maintained over the whole temperature range for these composites. This revealed the limitation of the

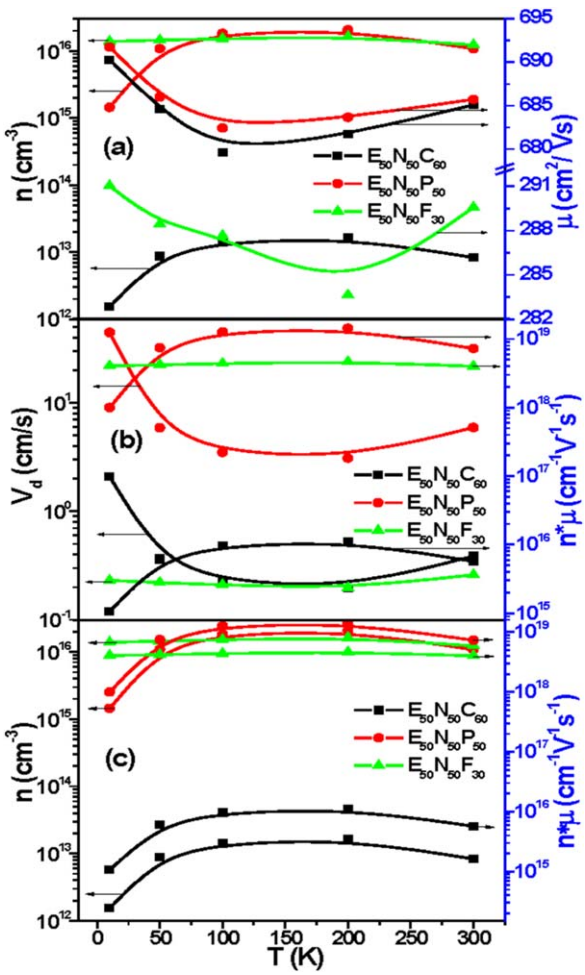

Figure 6. (a) n and μ versus temperature, (b) V_d and n $\times$ μ versus temperature, and (c) n and $n \times \mu$ versus temperature for the $E_{50}N_{50}C_{60}$, $E_{50}N_{50}P_{50}$, and $E_{50}N_{50}F_{30}$ composites. [Color figure can be viewed in the online issue, which is available at wileyonlinelibrary.com.]

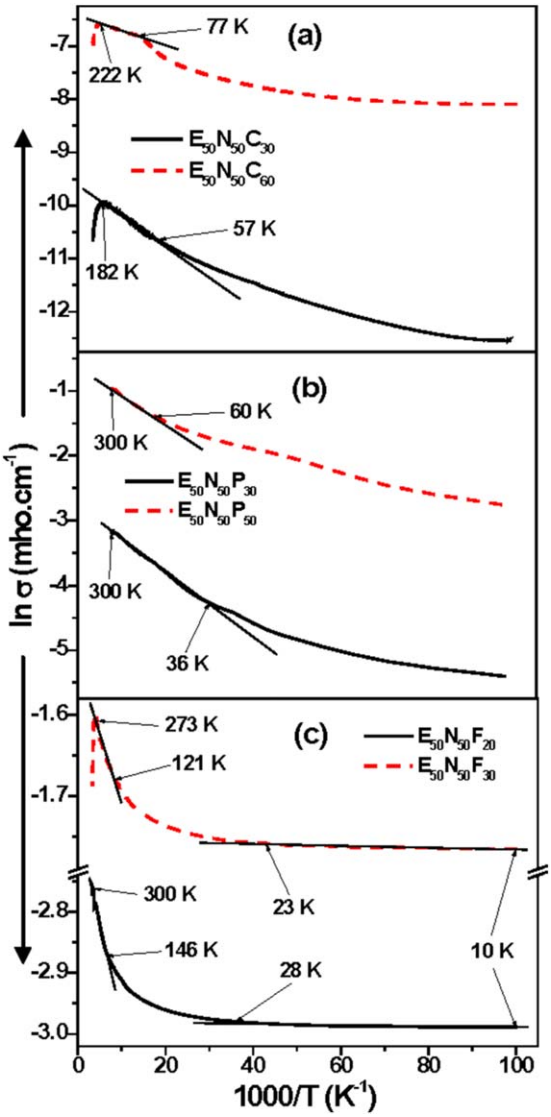

Figure 7. Applicability of the Arrhenius model for the (a) Conductex black, (b) Printex black, and (c) SCF-filled composites at different filler loadings. [Color figure can be viewed in the online issue, which is available at wileyonlinelibrary.com.]

Arrhenius model to describe the temperature-dependent conductivity in the low-temperature region. In fact, the Printex black filled composites exhibited applicability for the Arrhenius plot over a wider temperature range than the composites filled with Conductex black and SCFs.

The E_a values of conduction in a low-temperature region was estimated from the slopes of different plots and are presented in Table IV. We observed in the table that composites having higher filler loadings and higher conductivities exhibited lower E_a values. This was true for all of the composite systems under investigation. In fact, the ease of conduction depended on the ease of formation of a good conductive network with smaller average interparticle gaps, which could be easily hopped by electrons. The interparticle gap decreased with the conductive filler concentration and higher structure of carbon black. When the carbon filler had a higher aggregating tendency, it formed a more efficient conductive network, and E_a of the conductive composite also decreased. Moreover, E_a was found to be higher for the composite with a higher relative change in resistivity. However, the magnitude of E_a was related to the magnitude of the relative change in resistivity. The relative changes in resistivity for the Conductex carbon black filled composite (1–0.1) and Printex carbon black filled composite (1–0.2) were higher than that of the carbon-fiber-filled composites (1–0.8).

Kivelson Model. The power law behavior of temperature-dependent conductivity can also be explained by the Kivelson model. According to this law, the conductivity is a function of the temperature as follows[6,20,21]:

$$\sigma(T) = AT^n \tag{4}$$

or

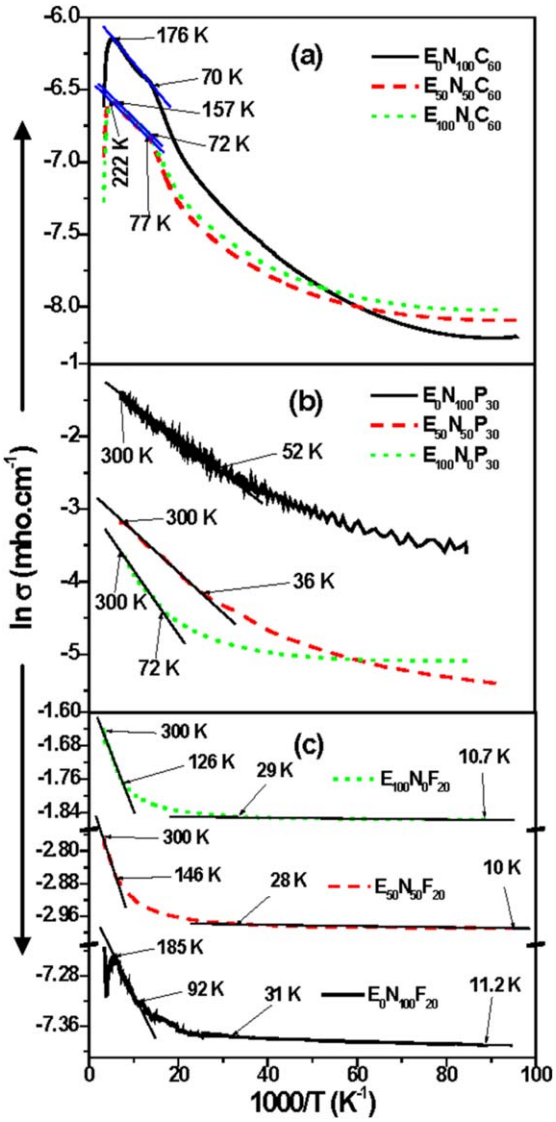

Figure 8. Applicability of the Arrhenius model for the (a) Conductex black, (b) Printex black, and (c) SCF-filled composites with different blend compositions. [Color figure can be viewed in the online issue, which is available at wileyonlinelibrary.com.]

Table IV. E_a Values of the Composites Filled with Different Carbon Fillers

Conductex black composites		Printex black composites		SCF composites	
Composite	E_a (meV)	Composite	E_a (meV)	Composite	E_a (meV)
$E_{50}N_{50}C_{30}$	2.98 ± 0.03	$E_{50}N_{50}P_{50}$	1.92 ± 0.02	$E_{50}N_{50}F_{30}$	0.215 ± 0.008
$E_0N_{100}C_{60}$	2.67 ± 0.02	$E_0N_{100}P_{30}$	2.69 ± 0.03	$E_0N_{100}F_{20}$	0.283 ± 0.011
$E_{50}N_{50}C_{60}$	2.11 ± 0.03	$E_{50}N_{50}P_{30}$	2.66 ± 0.03	$E_{50}N_{50}F_{20}$	0.324 ± 0.007
$E_{100}N_0C_{60}$	1.88 ± 0.02	$E_{100}N_0P_{30}$	2.35 ± 0.04	$E_{100}N_0F_{20}$	0.319 ± 0.009

$$\ln\sigma = \ln A + n \ln T \quad (5)$$

where A is a constant quantity and n is an exponent. The plot of $\ln\sigma$ versus $\ln T$ should be a straight line with a slope of n and an intercept of $\ln A$. Figures 9 and 10 show the plots of $\ln\sigma$ versus $\ln T$ for the composite systems based on different carbon fillers and blend compositions. We observed that the plots of $\ln\sigma$ versus $\ln T$ were mostly nonlinear in nature. It was thus apparent that this model also failed to predict the temperature-dependent conductivity over a wide range of temperatures. However, these plots were found to be linear over limited

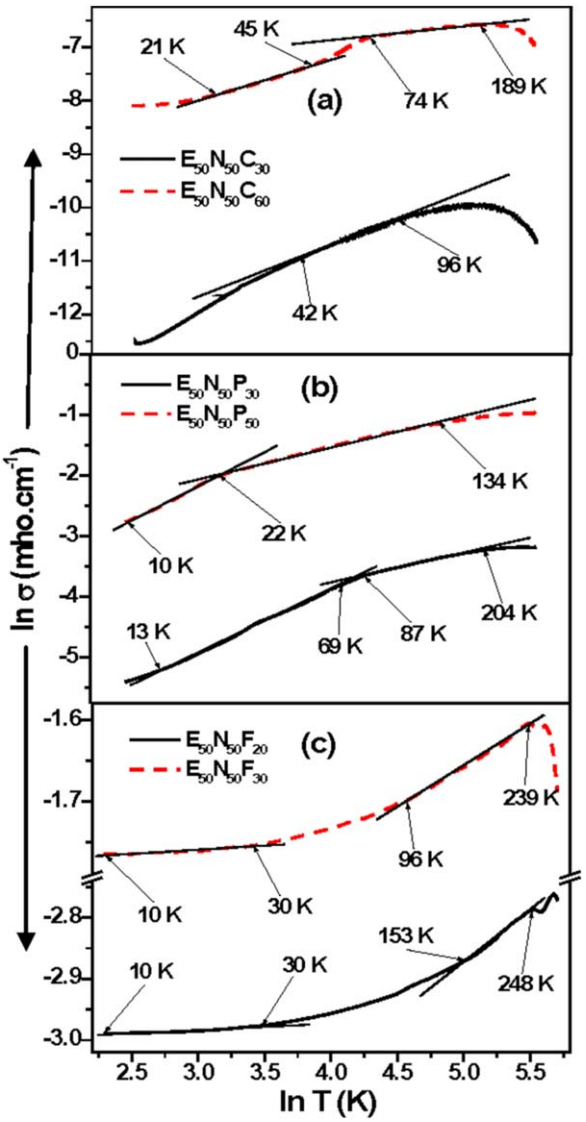

Figure 9. Applicability of the Kivelson model for the (a) Conductex black, (b) Printex black, and (c) SCF-filled composites at different filler loadings. [Color figure can be viewed in the online issue, which is available at wileyonlinelibrary.com.]

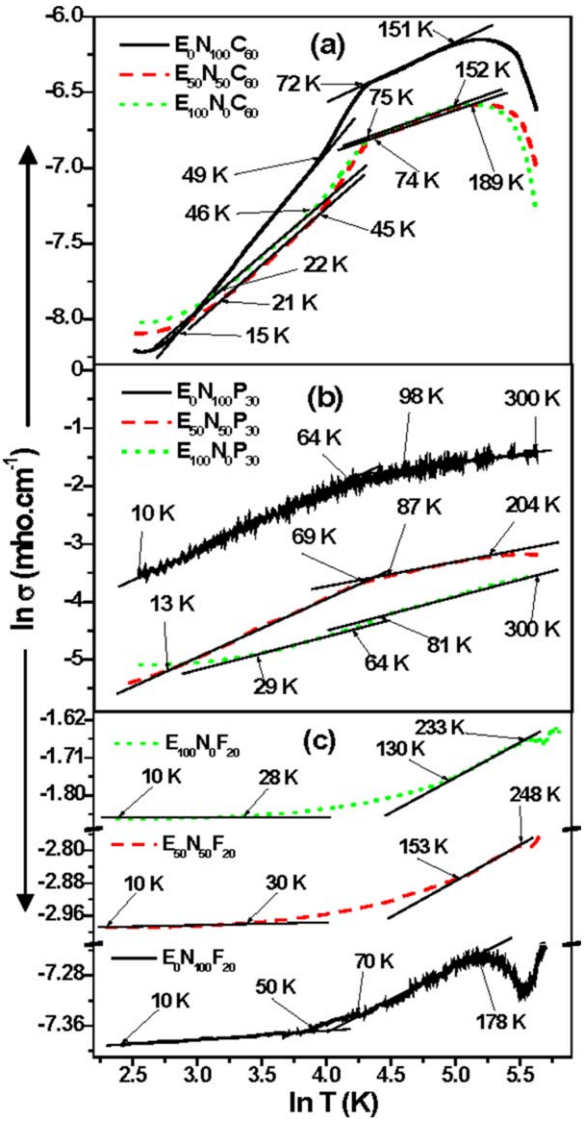

Figure 10. Applicability of the Kivelson model for the (a) Conductex black, (b) Printex black, and (c) SCF-filled composites with different blend compositions. [Color figure can be viewed in the online issue, which is available at wileyonlinelibrary.com.]

Table V. Values of Exponent n for the Composites Filled with Different Carbon Fillers

Conductex black composites		Printex black composites		SCF composites	
Composite	n	Composite	n	Composite	n
$E_{50}N_{50}C_{30}$	0.553 ± 0.004	$E_{50}N_{50}P_{50}$	0.435 ± 0.006	$E_{50}N_{50}F_{30}$	0.0612 ± 0.0012
$E_0N_{100}C_{60}$	0.514 ± 0.007	$E_0N_{100}P_{30}$	0.593 ± 0.007	$E_0N_{100}F_{20}$	0.0694 ± 0.0009
$E_{50}N_{50}C_{60}$	0.425 ± 0.006	$E_{50}N_{50}P_{30}$	0.574 ± 0.005	$E_{50}N_{50}F_{20}$	0.0876 ± 0.0013
$E_{100}N_0C_{60}$	0.347 ± 0.003	$E_{100}N_0P_{30}$	0.536 ± 0.004	$E_{100}N_0F_{20}$	0.0854 ± 0.0011

temperature ranges. Like the Arrhenius model, the Kivelson model was also more applicable to the Printex black filled composites compared to the Conductex black and SCF filled composites. The exponential nature of the change in resistivity against temperature for the composites with Printex black made them more suitable for applicability of the Arrhenius and Kivelson models compared to the Conductex and SCF filled composites.

The values of the exponent n for the composite systems filled with different carbon fillers are given in Table V. We observed from the table that the value of the exponent decreased with increasing filler loading in the composite systems. In fact the magnitude of exponents was correlated with the relative change in the resistivity. Here, the values of the exponent were obtained from the slope of eq. (5), and the magnitude of this slope depended on the relative change in the y-axis parameter with respect to the x-axis parameter. The magnitude of the slope was higher when the relative change in the y-axis parameter was higher. In this respect, the experimental results of the relative change in resistivity, which are shown in Figures 3 and 5, were in consistent with the results of the exponent given in Table V.

Mott's (VRH) Model. According to Mott,[6,22] the charge transport at low temperature may take place beyond the nearest neighbor through the VRH mechanism. In such cases, the temperature-dependent dc conductivity is expressed as follows:

$$\sigma(T)=\sigma_0 e^{\left[-\left(\frac{T_0}{T}\right)^{\gamma}\right]} \tag{6}$$

or

$$\ln\sigma=\ln\sigma_0-\left(\frac{T_0}{T}\right)^{\gamma} \tag{7}$$

where σ_0 is the limiting conductivity at infinite temperature, T_0 is Mott's characteristic temperature, and the exponent γ is related to the dimensionality (d) of the transport process through the equation $\gamma = 1/(1 + d)$, where $d = 1$, 2, and 3 for one-dimensional, two-dimensional, and three-dimensional transport processes, respectively. For these systems, the electrical conduction is three-dimensional, and hence, $\gamma = 1/4$. Thus, eq. (7) is reduced to

$$\ln\sigma=\ln\sigma_0-\left(\frac{T_0}{T}\right)^{\frac{1}{4}} \tag{8}$$

The plot of ln σ versus $T^{-1/4}$ on the basis of eq. (8) should be a straight line. Figures 11 and 12 show the plots of ln σ versus $T^{-1/4}$ for the composite systems on the basis of different filler loadings and blend compositions. The figures show that the plots based on this model were nonlinear like those of the Arrhenius and Kivelson models. The trend of variations was like that of the Arrhenius model. The only difference was in their applicability ranges. We observed from the figures that like earlier models, the applicability here also ranges for the Printex

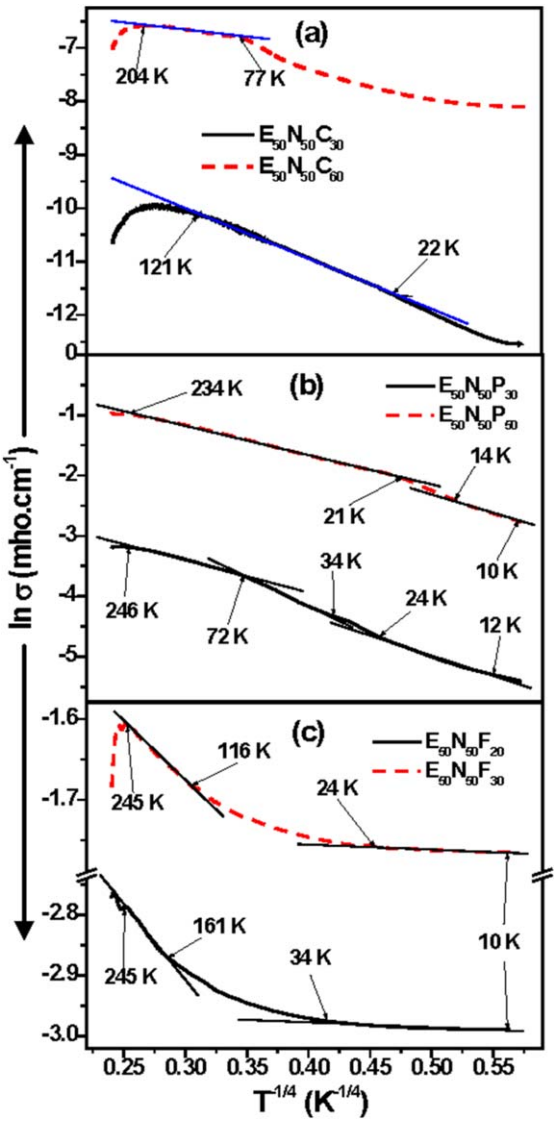

Figure 11. Applicability of Mott's model for the (a) Conductex black, (b) Printex black, and (c) SCF-filled composites at different filler loadings. [Color figure can be viewed in the online issue, which is available at wileyonlinelibrary.com.]

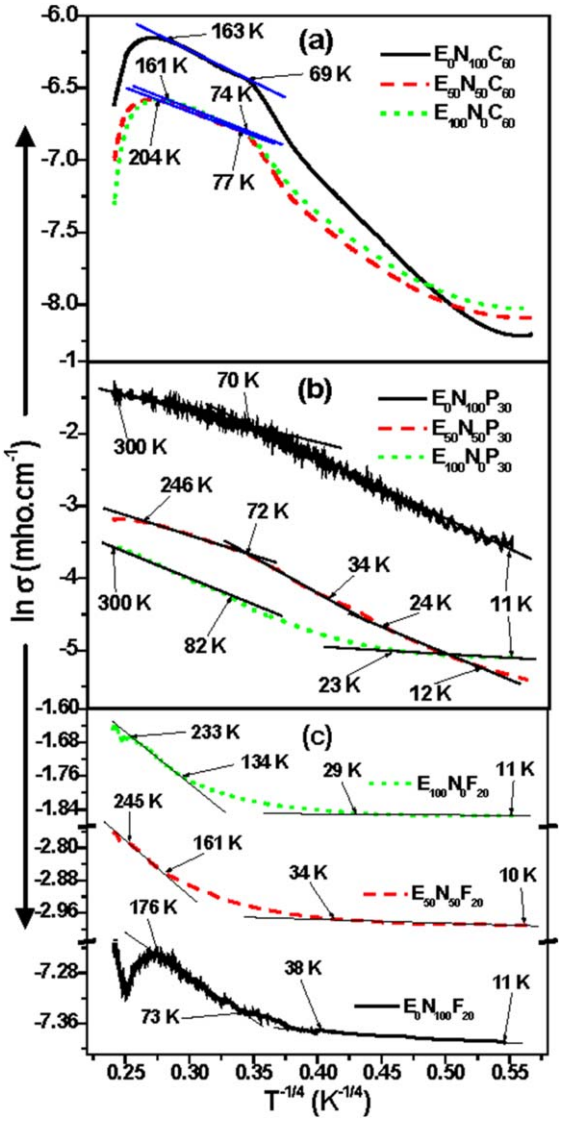

Figure 12. Applicability of Mott's model for the (a) Conductex black, (b) Printex black, and (c) SCF-filled composites with different blend compositions. [Color figure can be viewed in the online issue, which is available at wileyonlinelibrary.com.]

black filled composites were found to be wider compared to those of the other two composite systems.

T_0 was obtained from the slope of eq. (8) and is given in Table VI. The T_0 value was found to decrease with increasing filler loading for all of the composite systems. The trend of variation of T_0, exponent n, and E_a were similar to the respective composites. The only difference was in their magnitude.

Explanation for the Deviation of the Models. We mentioned earlier that the models were valid over a limited range of temperatures, and this range varied according to the nature of the polymers, the type of fillers, and the filler concentration. Actually, the electronic transport within the polymer matrix composites over a wide range of temperatures was governed by the thermal excitation, nearest neighbor hopping, VRH, and tunneling of electrons. The magnitude in all of these electronic transports through a composite material depended on the nature of the electronic path, which in turn, depended on the type of polymer, type of filler, and concentration of filler within the polymer matrix. As EVA was semicrystalline and NBR was amorphous with different viscosities, the dispersion of fillers, their breakdown, and the nature of the conductive electronic path within these two polymers was different. This means that the expectation of getting a similar temperature range validity of these models for the EVA and NBR composites for any type of filler was remote. When we changed the filler type and kept the polymer type and concentration of filler constant, we expected that the nature of the conductive electronic path within the polymer matrix would vary. This was because the carbons had different dimensions. The Conductex and Printex blacks were particulate fillers, and the SCFs were rodlike, as shown in Figure 13. Printex black had a higher structure compared to Conductex black, and hence, it formed a conductive electronic path with fewer numbers of contacts compared to Conductex black.[13,15] SCFs had a very high aspect ratio and, hence, formed a conductive electronic path with the lowest number of contacts.[14] Therefore, with the change in filler type, we obtained different temperature range validities for the models. Because of the lower numbers of electronic contacts among the SCFs within the polymer matrix, an almost linear dependence of dc resistivity was observed in the lower temperature range, whereas for both carbon blacks, the dc resistivity exhibited exponential dependence in a lower temperature region. The greater suitability of these models for the Printex black filled composite was due to its strong polymer–filler interaction compared to the others; this kept the conductive electronic path less disturbed with increasing temperature compared to the Conductex black and SCFs.[23] The increases in the filler loading within the polymer matrixes increased the number of electronic conductive paths, and hence, the nature of the electronic path was changed; this resulted in a decrease in the contact length. This led to a different temperature range validity of these models when the filler loading was increased.

Table VI. Values of T_0 for the Composites

Conductex black composites		Printex black composites		SCF composites	
Composite	T_0	Composite	T_0	Composite	T_0
$E_{50}N_{50}C_{30}$	2205 ± 115	$E_{50}N_{50}P_{50}$	677 ± 51	$E_{50}N_{50}F_{30}$	0.171 ± 0.007
$E_0N_{100}C_{60}$	1585 ± 87	$E_0N_{100}P_{30}$	2556 ± 124	$E_0N_{100}F_{20}$	0.221 ± 0.009
$E_{50}N_{50}C_{60}$	701 ± 46	$E_{50}N_{50}P_{30}$	1870 ± 96	$E_{50}N_{50}F_{20}$	0.861 ± 0.013
$E_{100}N_0C_{60}$	343 ± 34	$E_{100}N_0P_{30}$	1717 ± 92	$E_{100}N_0F_{20}$	0.791 ± 0.011

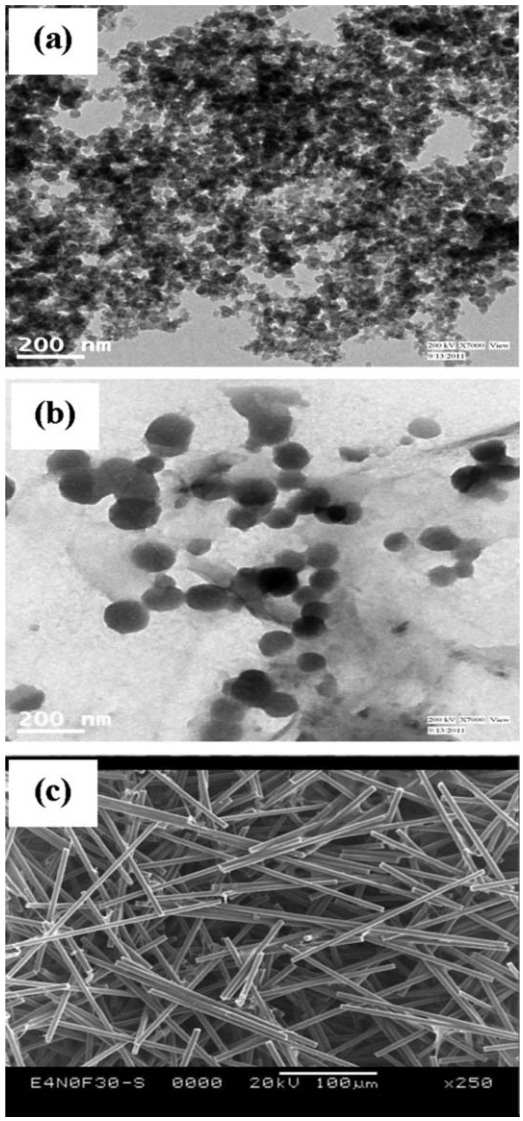

Figure 13. (a) Transmission electron microscopy image of the Conductex black, (b) transmission electron microscopy image of the Printex black, and (c) scanning electron microscopy image of SCF.

The Arrhenius model is based on the thermal excitation of charge carriers in which electronic transition takes place by the thermal activation of electrons. Thus, during the proposition of this model, the electronic transitions by nearest neighbor hopping, VRH hopping, and tunneling were not considered. These were the serious drawbacks of this model, and hence, these values were nonvalid over the wide range of temperatures. Although several linear ranges are shown in the figure, it can be argued that this model is applicable only in a higher temperature region, especially around the glass-transition region. This is because in a lower temperature region, the transport of electrons due to thermal activation almost ceased.[22]

Although the Kivelson model was proposed for the behavior of conductivity in the low-temperature region, it could not cover the whole temperature range for these composite systems. Actually, this model was developed to explain the electronic transport behavior of polyacetylene at a low temperature.[20,21] The electronic transition took place through a phonon-assisted tunneling/hopping process within the solitons. In the interchain transport process of polyacetylene, hopping occurred at the isoenergetic levels between the neutral and charged soliton states. The mobility of neutral solitons took place only along the carbon chain. So, in polyacetylene, interchain and along-the-chain charge transport took place, where the polymer was itself a semiconductor. However, for this composite system, we used two insulating polymers and their blend mixed with different types of conducting carbon fillers. Obviously, the natures of transport media in these composite systems were quite different compared to those of polyacetylene. Hence, this was one of the major reasons for the deviation of this model over the wide range of temperatures.

With Mott's VRH model, we plotted the conductivity versus temperature plots by considering the fact that the transport of charges within the polymer composites were three-dimensional in nature. This was logical in the sense that the carbons consisted of different graphitic layers of three-dimensional geometry. However, the charge transport across the two dimensions of a particular layer could not be ignored. Moreover, this model was proposed for amorphous semiconducting materials and doped polycrystalline semiconductors.[22] So, it was not obvious that it would be applicable for all types of materials and composite systems. Although different temperature ranges of validity are shown in the figure, it was mentioned in literature that Mott's VHR model is more applicable to the lower temperature region.[22] During the proposition of this model, the change transport through the thermal activation and tunneling of electrons was not considered. Finally, for polymer-filled conductive composites, there are different transitions, such as the glass-transition temperature, associated with them when they are heated thermally. The movement of the polymer chain and polymer side chain take place when the composite is heated thermally; this disturbs the conductive network and thereby changes the hopping distance. During the proposition of this model, this property of the materials was not considered, and hence, all of these models showed deviation over the wide range of temperatures.

Current-Voltage (*I*-V) Characteristics

The *I*–V characteristics of the EVA/NBR (50/50) blend composites filled with 60-phr Conductex carbon black, 30-phr Printex carbon black, and 20-phr SCF-filled composites are shown in Figure 14. As shown in Figure 14(a,b), for the Conductex and Printex carbon black filled composites, the *I*–V relationship was nonlinear at temperatures of 10 and 50 K. This strongly suggests that electrical conduction in this region was more nonohmic in nature. This is why the sharp decrease in the resistivity was observed in this region for these two carbon black systems [Figure 1(a,b)]. Figure 14(c) shows that the electrical conduction for the carbon-fiber-filled composites is ohmic in nature at all of the measurement temperatures. Thus, the electrical conduction was dominated by fiber–fiber contact through the polymer matrix. This accounted for the linear decrease in the resistivity with increasing temperature for this system [Figure 1(c)].

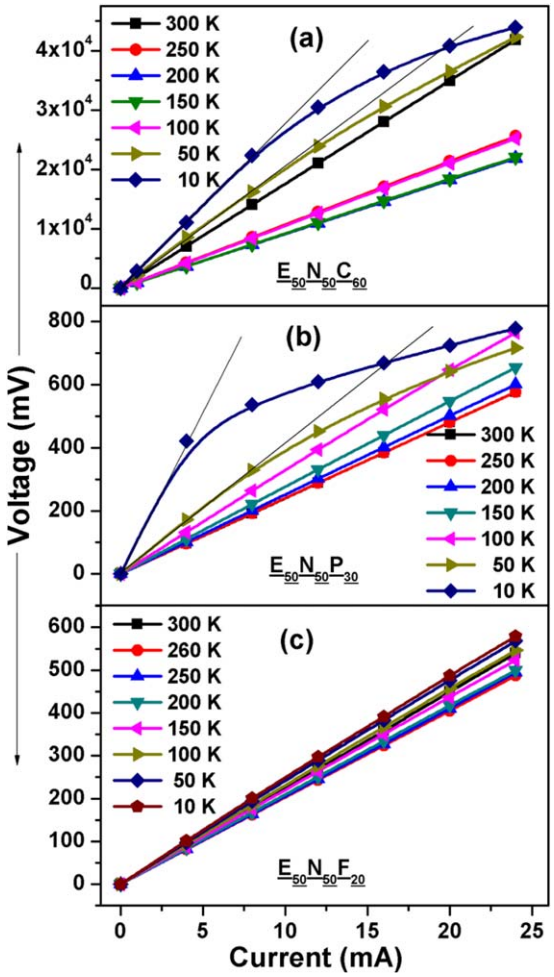

Figure 14. I–voltage characteristics of the (a) $E_{50}N_{50}C_{60}$, (b) $E_{50}N_{50}P_{30}$, and (c) $E_{50}N_{50}F_{20}$ composites. [Color figure can be viewed in the online issue, which is available at wileyonlinelibrary.com.]

CONCLUSIONS

At cryogenically low temperatures, where all molecular motion of the polymer chain is frozen, the conductivity of composites is mainly governed by the characteristics of conductive fillers. For carbon-black-filled composites containing Conductex and Printex carbon black, the resistivity decreased sharply over the temperature range from 10 K to around 60 K, and thereafter, the change in the resistivity with increasing temperature was marginal. Some tendency toward an increase in the resistivity against the temperature was observed beyond 250–260 K; this corresponded to the glass-transition temperatures of EVA and NBR. At these temperatures, some molecular motion of the polymer chain was set, and this affected the variation of the conductivity. However, for the SCF-filled composites, a linear decrease in the resistivity with increasing temperature was observed over the range 10–250 K, and thereafter, a peak was observed in the resistivity versus temperature plots. n and its μ were calculated with the Hall effect measurement. The applicability of three different models, namely, the Arrhenius, Kivelson, and Mott models, was tested to predict the temperature-dependent resistivity in the cryogenic temperature region. However, none of the three models was applicable to the entire range of measurement temperatures; rather, the validity of different models over limited temperatures was encountered. In fact, Mott's model was found to have better validity over an increased temperature range compared to other models discussed. The *I*–V characteristics revealed some nonohmic electrical conduction, especially at the lowest end of the temperature range, especially for the carbon-black-filled composites. However, ohmic conduction was observed for the carbon-fiber-filled composite.

ACKNOWLEDGMENTS

The authors thank the Aeronautic Research and Development Board, the Government of India, and the Deanship of Scientific Research at King Saud University for funding this research group (RG-1436-005).

REFERENCES

1. Klason, C.; Kubat, J. *J. Appl. Polym. Sci.* **1975**, *19*, 831.
2. Costa, L. C.; Henry, F. *J. Non-Cryst. Solids* **2011**, *357*, 1741.
3. Ghosh, P.; Ghatak, S.; Mandal, M. K.; Meikap, A. K. *Polym. Compos.* **2012**, *33*, 1941.
4. Bahrami, A.; Talib, Z. A.; Yunus, W. M. M.; Behzad, K.; Abdi, M. M.; Din, F. U. *Int. J. Mol. Sci.* **2012**, *13*, 14917.
5. Mzenda, V. M.; Goodman, S. A.; Auret, F. D. *Synth. Met.* **2002**, *127*, 285.
6. Kapil, A.; Taunk, M.; Chand, S. *J. Mater. Sci. Mater. Electron.* **2010**, *21*, 399.
7. Khissi, M.; Hasnaoui, M. E.; Belattar, J.; Graça, M. P. F.; Achour, M. E.; Costa, L. C. *J. Mater. Environ. Sci.* **2011**, *2*, 281.
8. Kapil, A.; Taunk, M.; Chand, S. *Asian J. Chem.* **2009**, *21*, S138.
9. Kattimani, J.; Sankarappa, T.; Praveenkumar, K.; Ashwajeet, J. S.; Ramanna, R.; Chandraprabha, G. B.; Sujatha, T. *Int. J. Adv. Res. Phys. Sci.* **2014**, *1*, 17.
10. Wang, Y.; Santiago-Avilés, J. *J. IEEE Trans. Nanotechnol.* **2004**, *3*, 221.
11. Li, Q.; Li, Y.; Zhang, X.; Chikkannanavar, S. B.; Zhao, Y.; Dangelewicz, A. M.; Zheng, L.; Doorn, S. K.; Jia, Q.; Peterson, D. E.; Arendt, P. N.; Zhu, Y. *Adv. Mater.* **2007**, *19*, 3358.
12. Yasin, S. F.; Zihlif, A. M.; Ragosta, G. *J. Mater. Sci. Mater. Electron.* **2005**, *16*, 63.
13. Rahaman, M.; Chaki, T. K.; Khastgir, D. *J. Mater. Sci.* **2011**, *46*, 3989.
14. Rahaman, M.; Chaki, T. K.; Khastgir, D. *Polym. Compos.* **2011**, *32*, 1790.
15. Rahaman, M.; Chaki, T. K.; Khastgir, D. *J. Mater. Sci.* **2013**, *48*, 7466.
16. Rahaman, M.; Chaki, T. K.; Khastgir, D. *Compos. Sci. Technol.* **2012**, *72*, 1575.

17. Ram, R.; Rahaman, M.; Khastgir, D. *Compos. A* **2015**, *69*, 30.
18. Sau, K. P.; Chaki, T. K.; Khastgir, D. *Polymer* **1998**, *39*, 6461.
19. Tawalbeh, T. M.; Saqan, S.; Yasin, S. F.; Zihlif, A. M.; Ragosta, G. *J. Mater. Sci. Mater. Electron.* **2005**, *16*, 351.
20. Kivelson, S. *Mol. Cryst. Liq. Cryst.* **1981**, *77*, 65.
21. Kivelson, S. *Phys. Rev. B* **1982**, *25*, 3798.
22. Park, J.; Mitchel, W. C.; Elhamri, S.; Grazulis, L.; Altfeder, I. *Phys. Rev. B* **2013**, *88*, 035419.
23. Rahaman, M. Ph.D. Thesis, Indian Institute of Technology Kharagpur, 2015.